MLM-2860(OP)

CONF-810926--5

SURFACE STUDIES OF PLASTIC-BONDED PETN AND RDX BY X-RAY PHOTOELECTRON SPECTROSCOPY (XPS) AND ION-SCATTERING SPECTROSCOPY (ISS)

P. S. Wang, W. E. Moddeman, L. D. Haws
Monsanto Research Corporation
Mound Facility*
Miamisburg, Ohio

and

T. N. Wittberg, J. A. Peters
University of Dayton Research Institute
Dayton, Ohio

ABSTRACT

Surface structures of plastic bonded PETN and RDX were studied by high resolution X-Ray Photoelectron Spectroscopy (XPS) and Ion Scattering Spectroscopy (ISS). The coating material is a copolymer of vinyl chloride and chlorotrifluoroethylene. Specimens with 6 wt % of the coating on RDX and 4 wt % on PETN were used in these studies.

High resolution elemented XPS spectra of F 1s, N 1s, C 1s, and Cl 2p indicate that the surface of coated RDX (PBX-9407) is covered and the coating film is thicker than 100Å; the results with coated PETN (LX-16) show the surface layer to be thinner than 100Å. $^{3}He^{+}$ ISS data on LX-16 suggest that the coating on PETN is not uniform and is, in fact, absent in some regions.

*Mound Facility is operated by Monsanto Research Corporation for the United States Department of Energy under Contract No. DE-AC04-76-DP00053.

DISCLAIMER

INTRODUCTION

Surface studies of plastic bonded explosives (PBX) have been conducted by XPS and ISS. The reasons for coating a chosen explosive powder with a specific surface binder are:

1. to improve the mechanical strength of the powders and thus increase the rigidity of the pellets into which the powders are pressed;

2. to control the physical characteristics of the powder surfaces for easy handling;

3. to maximize the energy output of the explosive per unit volume; and

4. to control the sensitivity of the explosive for safety or other reasons.

Whether the above advantages can be achieved depends critically upon the choice of the binder for a specific explosive, the percentage of the binder, and the thickness as well as the uniformity of the coating in PBX composites.

If the chosen explosive has both a high surface energy and a specified number of acidic sites, the ideal binder to form a PBX would be one with roughly an equivalent surface energy and a complementary basicity [1,2]. It is also believed that in order to minimize the sensitivity of the composite, a low modulus coating should be used, otherwise a stiff, crack-susceptible, highly sensitive composite will be formed [1,3].

XPS, a surface sensitive technique, has been applied to analyze the surface coating of explosives with a certain degree of success. However, the overall application of this method to PBX was found to be doubtful [4]. The

factors contributing to this limitation are:

1. sample charging due to the insulation inherent in organic samples; and

2. relatively limited resolution of XPS with respect to the small binding energy differences in carbon and oxygen.

In this paper, we have re-examined the applicability not only of XPS, but also of ISS, to the surface analysis of explosives and PBX's. We have chosen two PBX's which illustrate the methodology. One PBX was completely, the other incompletely, coated.

EXPERIMENTAL

Samples

Pentaerythritol tetranitrate (PETN, $C_5H_8N_4O_{12}$) and 1,3,5 - trinitro - 1,3,5 - triazacyclohexane (RDX, $C_3H_6N_6O_6$) are the explosives of our study. Their molecular structures are:

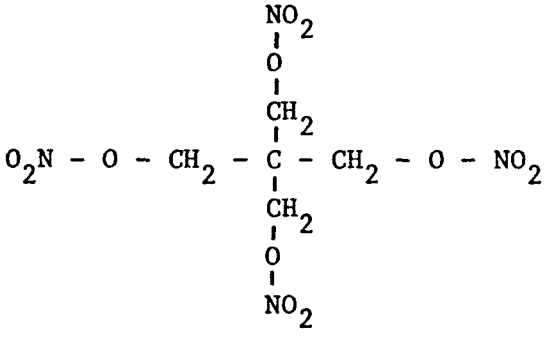

PETN

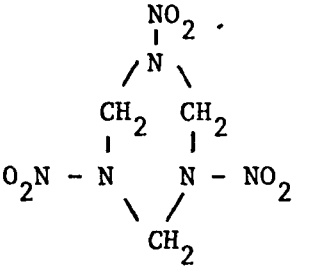

RDX

The coating material of both PBX's (LX-16 and PBX-9407) is a copolymer of vinyl chloride and trifluorochloroethylene (trade named FPC 461), which has the following structure:

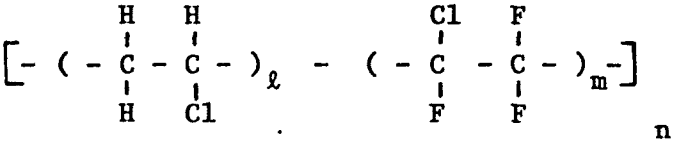

PBX-9407 was purchased from Holston; its composition is 94 wt % RDX and 6 wt % FPC 461. LX-16 was processed at Mound (ER7364A); its composition is 96 wt % PETN and 4 wt % FPC 461. A small amount of each sample was sprinkled on a piece of Fullum copper adhesive tape prior to spectroscopic analysis.

Spectrometers

ISS spectra were obtained with a 3M Model 525 ion scattering spectrometer which uses a 138^{o} backscatter collection geometry. In this system a 3M minibeam ion gun is concentric with a single pass cylindrical mirror analyzer. Spectra were recorded using an incident ion beam of $^{3}He^{+}$ at an energy of 2500 eV. The spectrometer was backfilled with ^{3}He to 5×10^{-5} torr. A charge neutralization filament was used to provide a source of low energy electrons to reduce the effects of positive charge buildup on the nonconductive specimen.

The XPS spectrometer is a modified AEI ES-100 instrument. This spectrometer with the accompanying argon ion sputtering system is pumped by a 110 liter/sec ion pump and a 220 liter/sec turbomolecular pump. The vacuum achievable in the sample chamber is 10^{-8} torr. The anode used for all the XPS measurements was magnesium.

RESULTS AND DISCUSSION

Illustrated in Figures 1, 2, and 3 respectively, are the overall XPS spectra of PETN (the explosive), FPC 461 (the coating), and LX-16 (PBX composite). Nitrogen, oxygen, and carbon were detected in PETN, as expected; fluorine, chlorine, oxygen, and carbon were detected in FPC 461. In the LX-16 sample, all these elements were observed. In Figure 4, high resolution F 1s and Cl 2p XPS spectra of these three samples are shown. These two signals can be observed at binding energies of 689.2 eV and 203.4 eV, respectively, in both FPC 461 and LX-16. No F or Cl signals were observed for PETN. The most interesting XPS data are the C 1s signals which are shown in Figure 5. Figure 5(a) indicates that in PETN, three types of carbon at binding energies of 285.4 eV, 287.2 eV, and 289.6 eV with respective signal areas of 22%, 64% and 14% were observed. These signals can be primarily attributed to the carbon of the $-\dot{C}-$ bond, of the $-CH_2-$ groups, and of contaminants containing CO_x groups, respectively. In PETN, the theoretical ratio of $-CH_2-$ groups to $-\dot{C}-$ bonds should be 4; we observed 3. Figure 5(c) illustrates the C 1s signal of FPC 461; no residual carbon impurity was observed. This signal can be deconvoluted into three peaks at 286.5 eV, 289.0 eV and 292.3 eV with relative intensities of 45%, 29% and 26%, respectively. The highest binding energy peak is due to $-CF_2-$; the peak at 289.0 eV is due to the -CFCl-; and the lowest binding energy is probably due to the sum of $-CH_2-$ and -CHCl- groups. These assignments agree closely with theoretical values based on the formula of the binder being $[(-CF_2CFCl-)_3-(-CH_2CHCl-)_2]$. Figure 5(b) shows C 1s XPS of LX-16. The peak at 285.6 eV indicates surface contaminant of residual carbon remaining on the surface of the PBX; probably this residual carbon is toluene, the solvent used in dissolving FPC 461 during coating. The peaks at 292.1 eV (18% of total signal) and 289.8 eV (19% of total signal) can be assigned to $-CF_2-$ and -CFCl- of the plastic. The peak at 287.6 eV (38% of total signal) can be interpreted as a combination of $-CH_2-$ of PETN and $-CH_2CHCl-$ of FPC 461. The fact that the intensity ratios of

the photopeak at 287.6 eV to that of both the 292.1 eV and 289.8 eV signals are $\sim$ 1 rather than 1.5 suggests that the $-CH_2-$ of the PETN contributes part of the 287.6 eV peak. These data on the composite can be explained as follows:

1. The plastic coating film thickness of the LX-16 composite is less than the C 1s photoelectron mean free path which is $\sim$100Å for a 970 eV electron; and/or

2. The plastic coating on the PETN particles is incomplete.

The C 1s XPS data of PETN, FPC 461, and LX-16 are listed in Table 1.

These two possible explanations are supported by the N 1s XPS data given in Figure 6. The binding energy of the N 1s from the PETN is 408.2 eV as shown in Figure 6(a). Weak peaks at 399.8 eV and 398.0 eV are satellite signals that can be associated with the main peak at 408.2 eV. The fact that an N 1s signal was also observed in an LX-16 sample, as shown in Figure 6(b), is evidence that the surface coating is either thinner than 100Å, or incomplete, or both.

Figure 6 shows that the signals in the satellite region are broader in the composite (b) than in the PETN (a). This change in peak shape indicates that a new nitrogen structure at $\sim$ 400.3 eV binding energy is present in the composite but not in the explosive. Three N 1s spectra from an LX-16 sample that has been irradiated with Mg X-rays for an extended period of time is shown in Figure 7. These results show that X-ray induced decomposition of PETN forms the new structure at a binding energy of 400.3 eV. Possible nitrogen structures observed at this binding energy are $C-NH_2$ or C-N=N-C.

Residual gas analysis (RGA) of LX-16 during irradiation showed the main gaseous products to be 30, 44, 46, and 76 a.m.u. The possible assignments for these products are as follows:

30 - NO, C_2H_6
44 - CO_2, N_2O
46 - NO_2
76 - CH_2-O-NO_2

The most intense peak was observed at mass =30.

The time dependence of PETN decomposition is given in Table 2 and is plotted in Figure 8. These data show the X-ray induced decomposition of LX-16 to be a first-order process. Figure 9 illustrates a plot of the C 1s and O 1s signals ratioed to the N 1s signal. These data show nitrogen decreasing more rapidly than carbon or oxygen as the time of X-irradiation increases. Table 3 lists the data plotted in Figure 9. We conclude from the RGA and XPS data taken during X-irradiation that (1) nitrogen-containing gaseous components evolve from the PETN and (2) the surface, after X-ray degradation, is enriched in carbon and oxygen.

With ISS the composition of the outermost atomic layer of a sample surface can be determined. With this technique a sample is bombarded with a beam of noble gas ions, and some of these ions will experience binary elastic collisions with surface atoms. From the laws of conservation of momentum and energy, the energy of these scattered primary ions can be computed in terms of the masses of the sample atoms, the probe ions, and the scattering angle. By measuring the ratio of scattered primary ion energy (E) to primary ion energy (Eo), the mass of the sample atoms can be determined.

The probe gas used for ISS measurements was $^3He^+$ at 2.5 KeV energy. The sputter rate with $^3He^+$ is very low, probably about 1Å/min. Two different areas of an LX-16 specimen were analyzed and, in both instances, the ion beam covered several particles. The ISS data given in Figure 10 are representative of one of the two areas where the sample has been exposed to 5, 10, 12, and 45 min of $^3He^+$ exposure. In both cases, the elements fluorine, oxygen, and nitrogen were detected initially. Exposing for longer periods of time did not change the relative amounts of these elements appreciably.

The scan taken after 45 min of exposure on the first spot did show a slight increase in the carbon energy region. The initial detection of the N signal in the coated powder suggests that the surface of LX-16 powders are not completely coated with FPC 461. This is possibly due to the low percentage (only 4%) of coating material used in the manufacturing of the LX-16 composite.

There are a couple of points about the data which are not explainable at this time. First, chlorine was detected using XPS, yet it was not detected with ISS. It should appear at $E/E_o \doteq 0.74$. Secondly, very little carbon was detected with ISS. It could be that these elements actually are not present in the first few monolayers, although this does not seem likely.

XPS spectra data of F 1s, N 1s, C 1s and Cl 2p were recorded on each of three samples of FPC 461, RDX and PBX-9407 and tabulated in Table 4. Representative spectra of N 1s are shown in Figure 11; Cl 2p and F 1s are shown in Figure 12. No N signal was observed from the FPC 461 and PBX-9407 samples; however, C, Cl and F signals were identified. As expected, no Cl and F peaks were seen with the RDX sample.

CONCLUSIONS

The data presented in this text show that XPS and ISS can successfully be used in measuring the surface structure, the thickness, and the completeness of plastic coated explosives. From the XPS and ISS data for the LX-16 sample, it was concluded that the coating on the LX-16 particles is not uniform and is in fact, absent in some regions. From the XPS data on PBX-9407, it was concluded that the substrate RDX explosive is coated. Since the mean free path of a C 1s photoelectron in organic materials is >100Å and since no N 1s signal could be observed with this PBX-9407, the thickness of the coating on RDX in the composite is concluded to be >100Å.

REFERENCES

1. J. K. Bower, J. R. Kolb, and C. O. Pruneda, Industrial Engineering Chemistry, Product Research Development, Volume 19, 326 (1980).

2. F. M. Fowkes, M. A. Mostafa, Industrial Engineering Chemistry, Product Research Development, Volume 17, 3 (1978).

3. P. S. Wang, friction sensitivity of LX-16, unpublished data.

4. H. R. Borlace, D. J. Prince, Proceedings SUBWOG 12, May 1978.

5. T. N. Wittberg, J. R. Hoenigman, W. E. Moddeman, C. R. Cothern, and M. R. Gulett, J. Vac. Sci. Technol., Volume 15, 348 (1978).

TABLE 1

XPS Data for C 1s in PETN, LX-16, and FPC 461

Sample	Binding Energy (eV)	Intensity (%)	Identification
PETN	285.4	22.0	(-C(-)-)
	287.2	64.0	$-CH_2-$
	289.6	14.0	(CO_x)
FPC 461	286.5	45	-CHCl- and $-CH_2-$
	289.0	29	-CFCl-
	292.3	26	$-CF_2-$
LX-16	285.6	25	(-C(-)-) and Residual carbon
	287.6	38	$-CH_2-$ and -CHCl-
	289.8	19	(CO_x) and -CFCl-
	292.1	18	$-CF_2-$

TABLE 2

PETN decomposition and new nitrogen-containing product formation in LX-16 induced by X-irradiation

Time of X-irradiation (min)	$\frac{I_N 408}{I_N 400}$	$\ln \frac{I_N 408}{I_N 400}$
29	8.1	2.09
79	7.3	1.99
129	5.2	1.65
179	3.0	1.10
229	2.2	0.80
279	1.7	0.53
367	1.1	0.04

TABLE 3

Nitrogen change in PETN surface induced by X-irradiation

Time of X-irradiation (min)	$\frac{I_C(286)}{I_N}$	$\frac{I_O(O1s)}{I_N}$
24	1.15	4.77
177	1.55	5.50
250	1.98	6.99
326	2.32	9.25

TABLE 4
XPS data on FPC 461, RDX, and PBX-9407

Element and Level	Identification	FPC 461		RDX		PBX-9407	
		Binding Energy (eV)	Intensity (F=1)	Binding Energy (eV)	Intensity (F=1)	Binding Energy (eV)	Intensi (F=1)
F 1s	C-F	689.6	1	--	--	689.3	1
Cl 2p	C-Cl	203.0	1.05	--	--	202.6	0.70
N 1s	C C \N/	--	--	401.2	--	--	--
	O O \N/	--	--	406.9	--	--	--
C 1s	C-C (residual)	285.0	0.71	285.0	--	285.0	2.15
	CH_2	286.5	0.92	--	--	286.0	7.76
	C-Cl	287.7	1.21	287.7(?)	--	287.0	8.23
	C-ClF	289.3	0.83	--	--	288.5	5.37
						289.8	4.77
	CF_2	292.1	0.67	--	--	--	--

FIGURE CAPTIONS

1. Overall XPS spectrum of PETN.

2. Overall XPS spectrum of FPC 461.

3. Overall XPS spectrum of LX-16.

4. F 1s and Cl 2p spectra of (a) PETN
   (b) LX-16
   (c) FPC 461

5. C 1s XPS spectra of (a) PETN
   (b) LX-16
   (c) FPC 461

6. N 1s XPS spectra of (a) PETN
   (b) LX-16
   (c) FPC 461

7. N 1s XPS spectra of LX-16 caused by different degree of X-ray decomposition.

8. N 1s XPS intensity changes due to Mg anode irradiation in LX-16.

9. Nitrogen decrease in LX-16 during X-irradiation.

10. ISS of LX-16.

11. N 1s XPS spectra of (a) RDX
    (b) PBX-9407
    (c) FPC 461

12. Cl 2p and F 1s XPS spectra of (a) FPC 461
    (b) RDX
    (c) PBX-9407

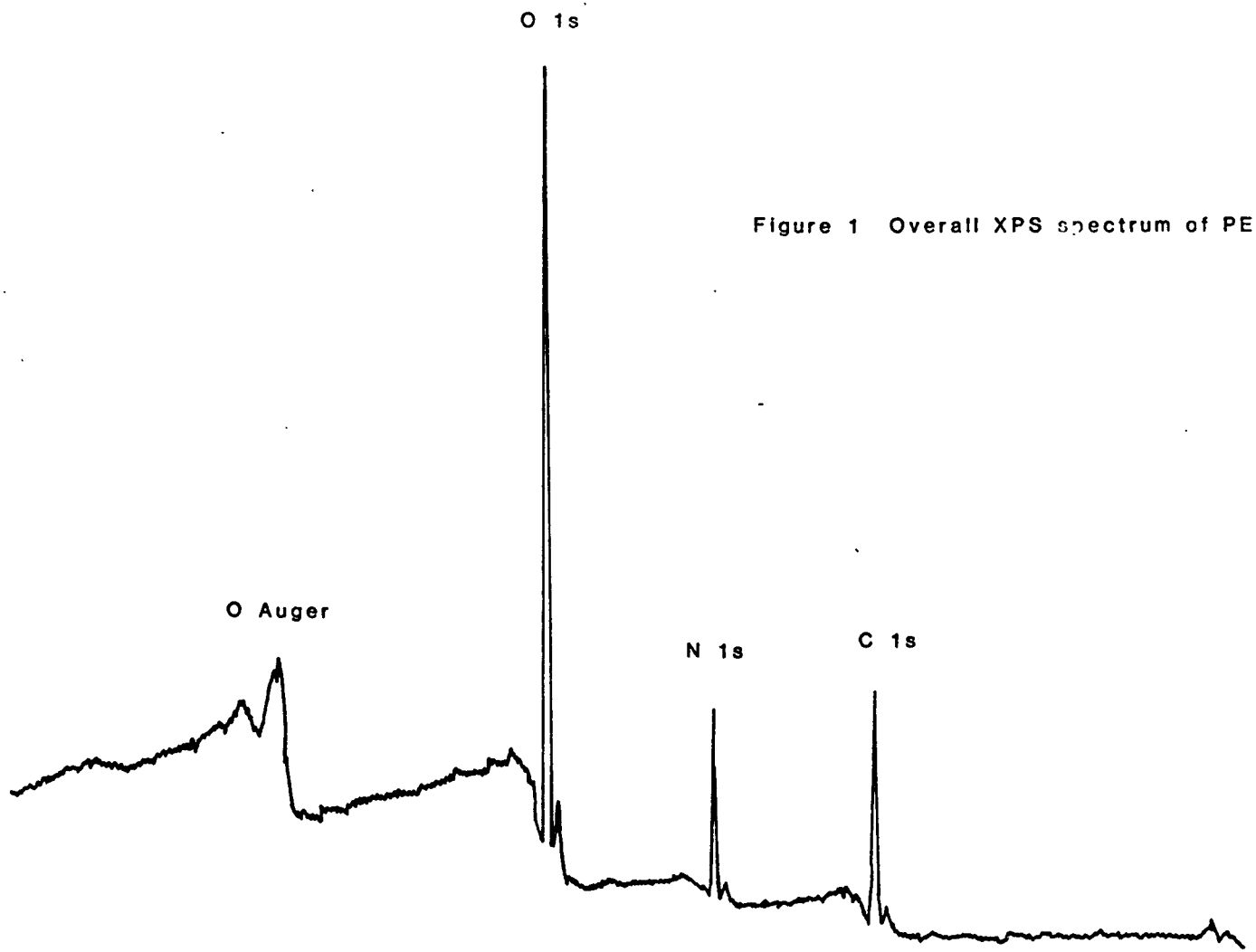

Figure 1 Overall XPS spectrum of PETN

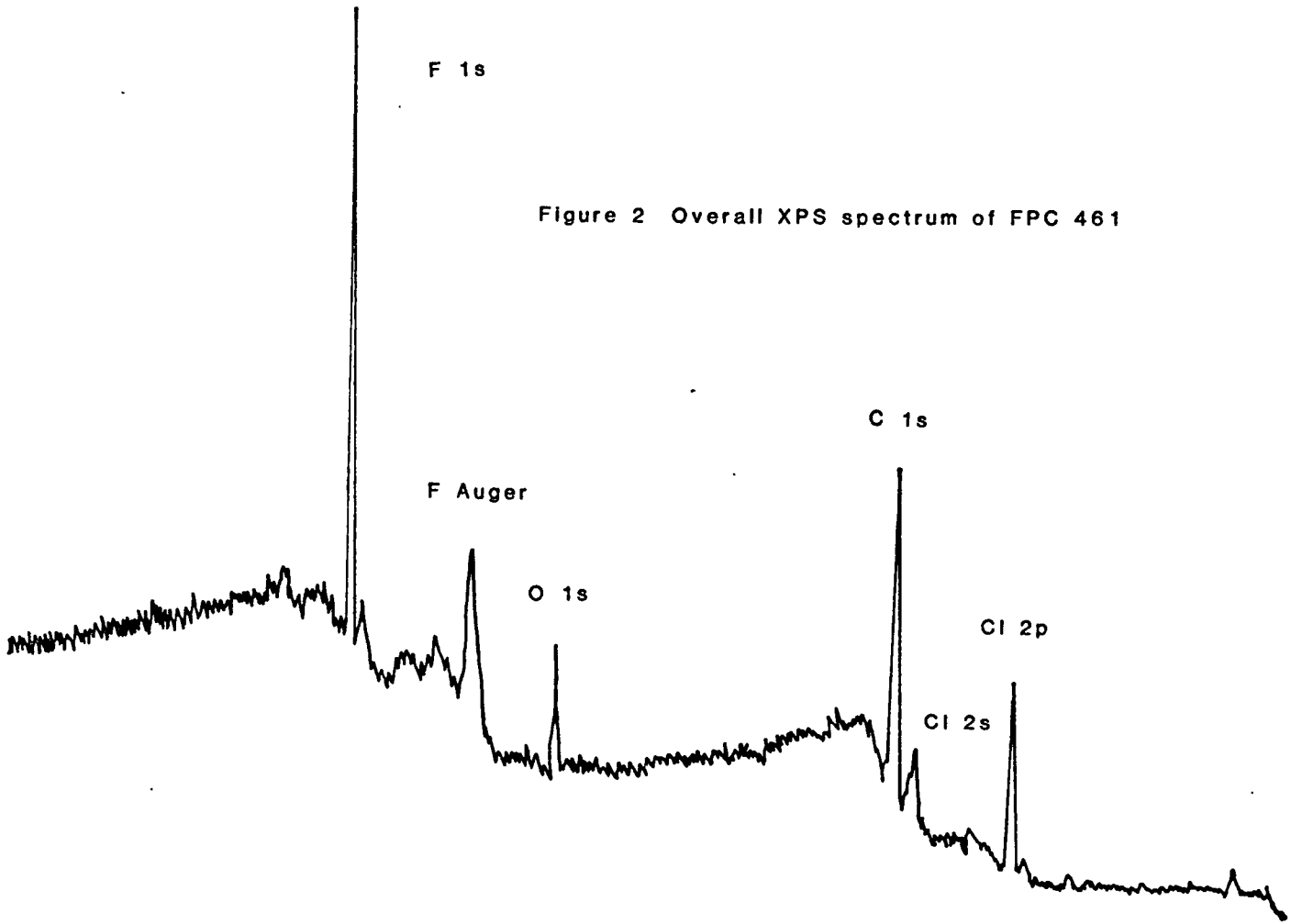

Figure 2 Overall XPS spectrum of FPC 461

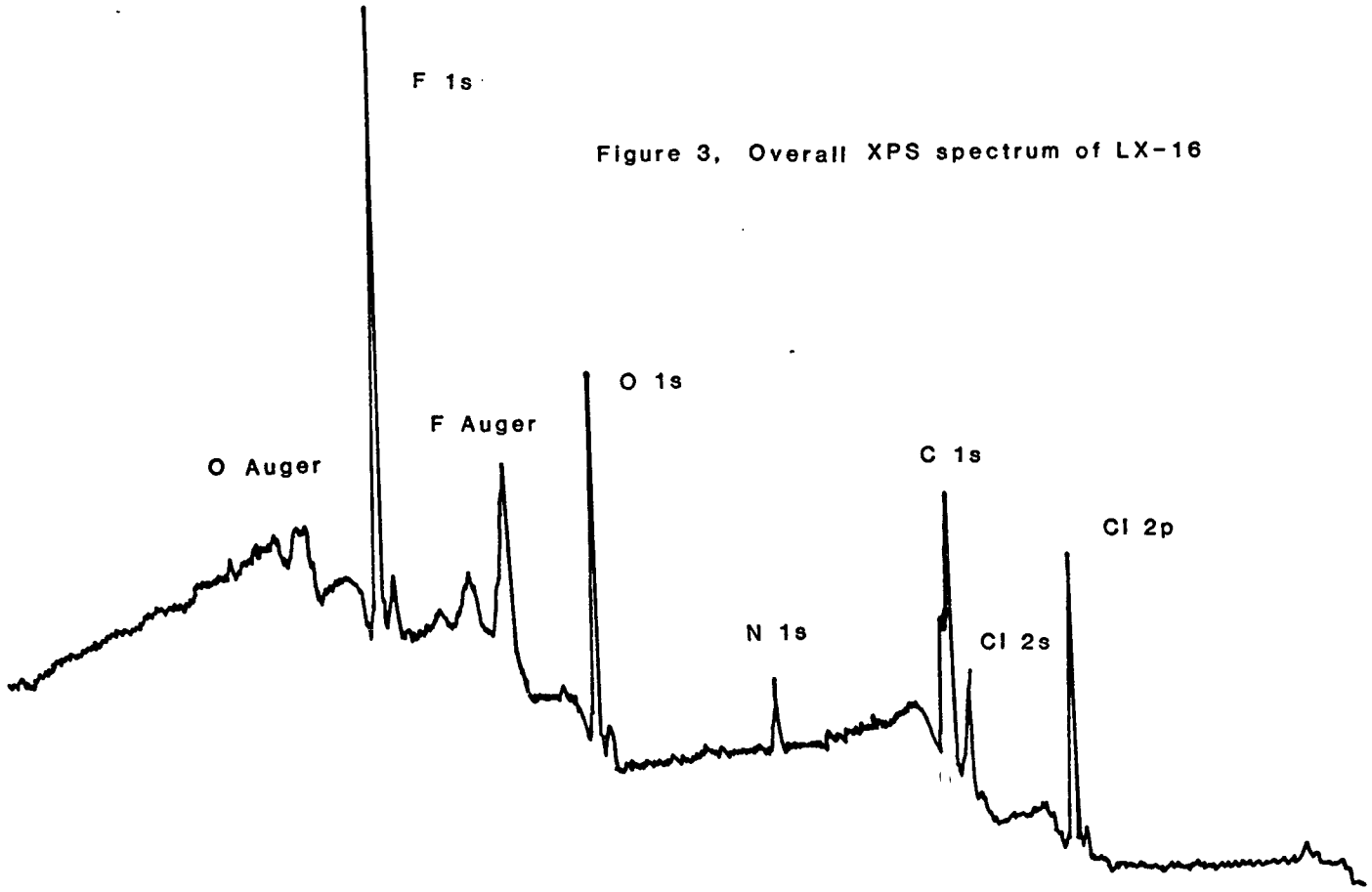

Figure 3, Overall XPS spectrum of LX-16

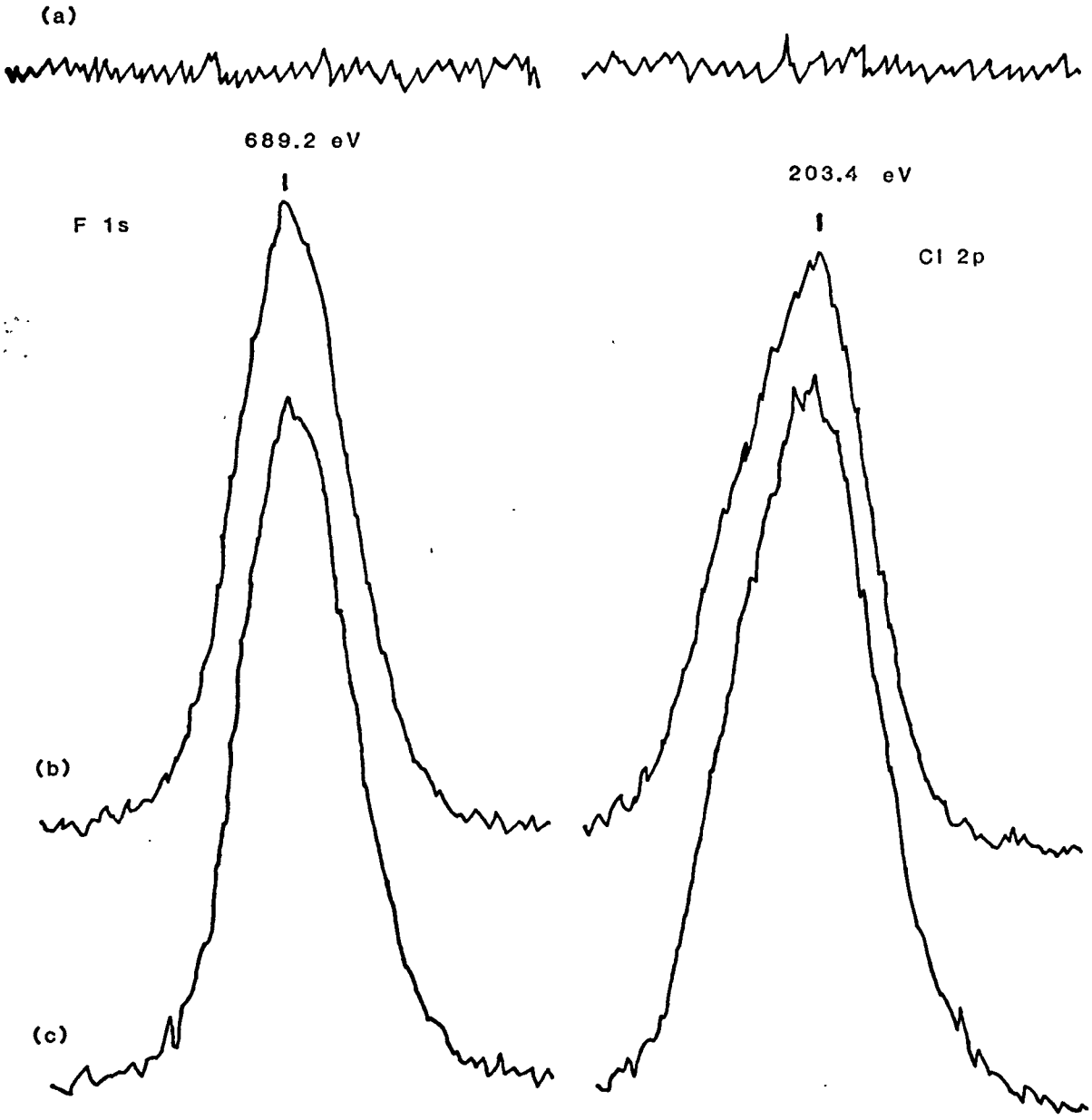

Figure 4 F 1s and Cl 2p XPS spectra of (a) PETN
(b) LX-16
(c) FPC 461

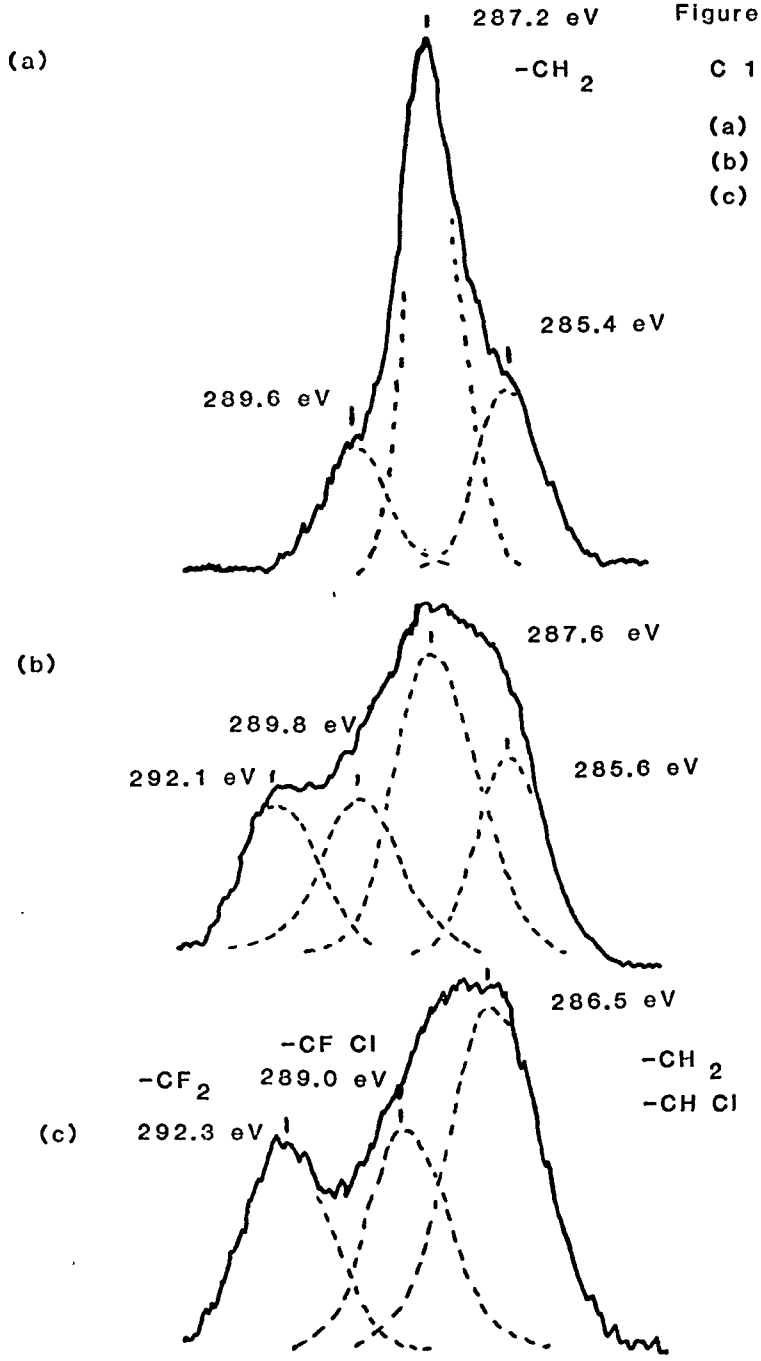

Figure 5

C 1s XPS spectra of

(a) PETN
(b) LX-16
(c) FPC - 461

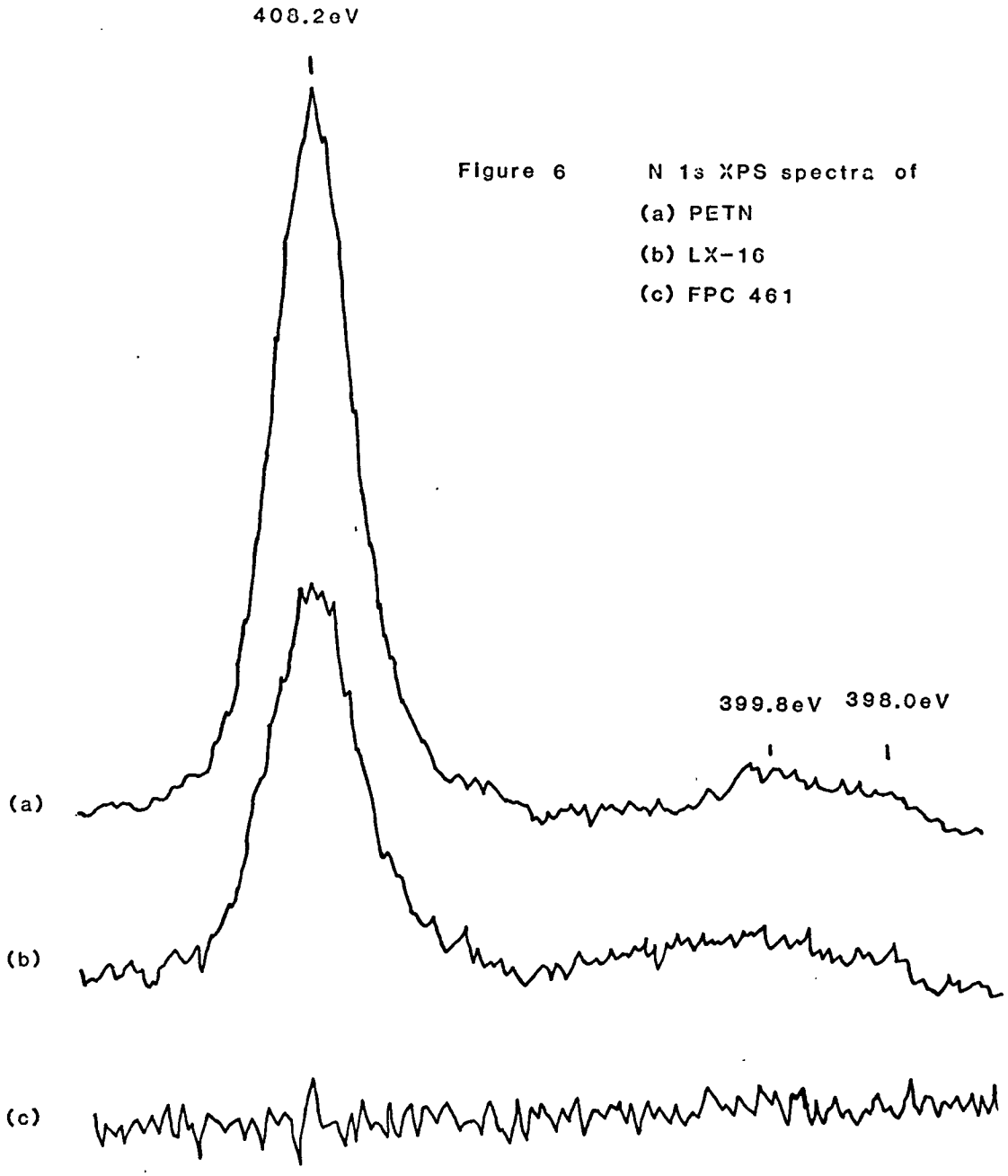

Figure 6 N 1s XPS spectra of
(a) PETN
(b) LX-16
(c) FPC 461

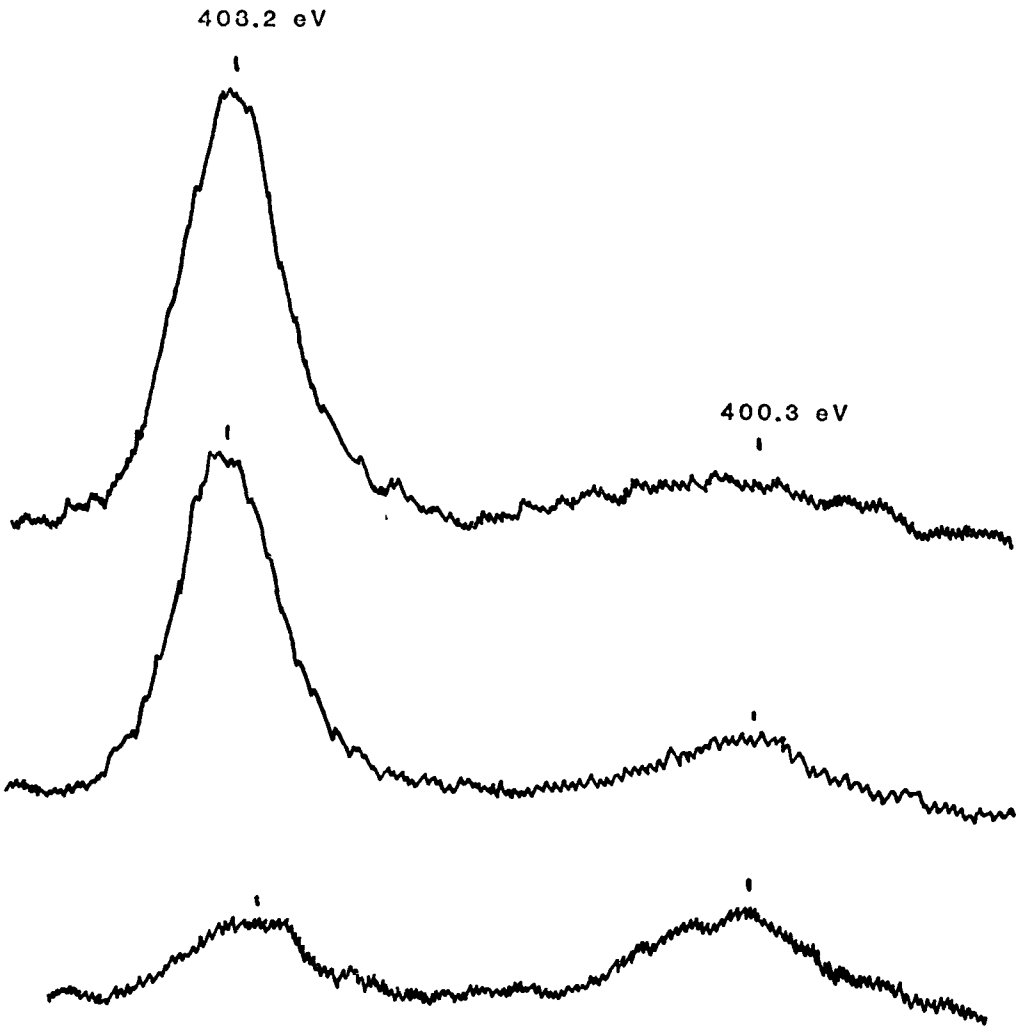

Figure 7 N 1s XPS spectra of LX-16 caused by different degree of x-ray decomposition

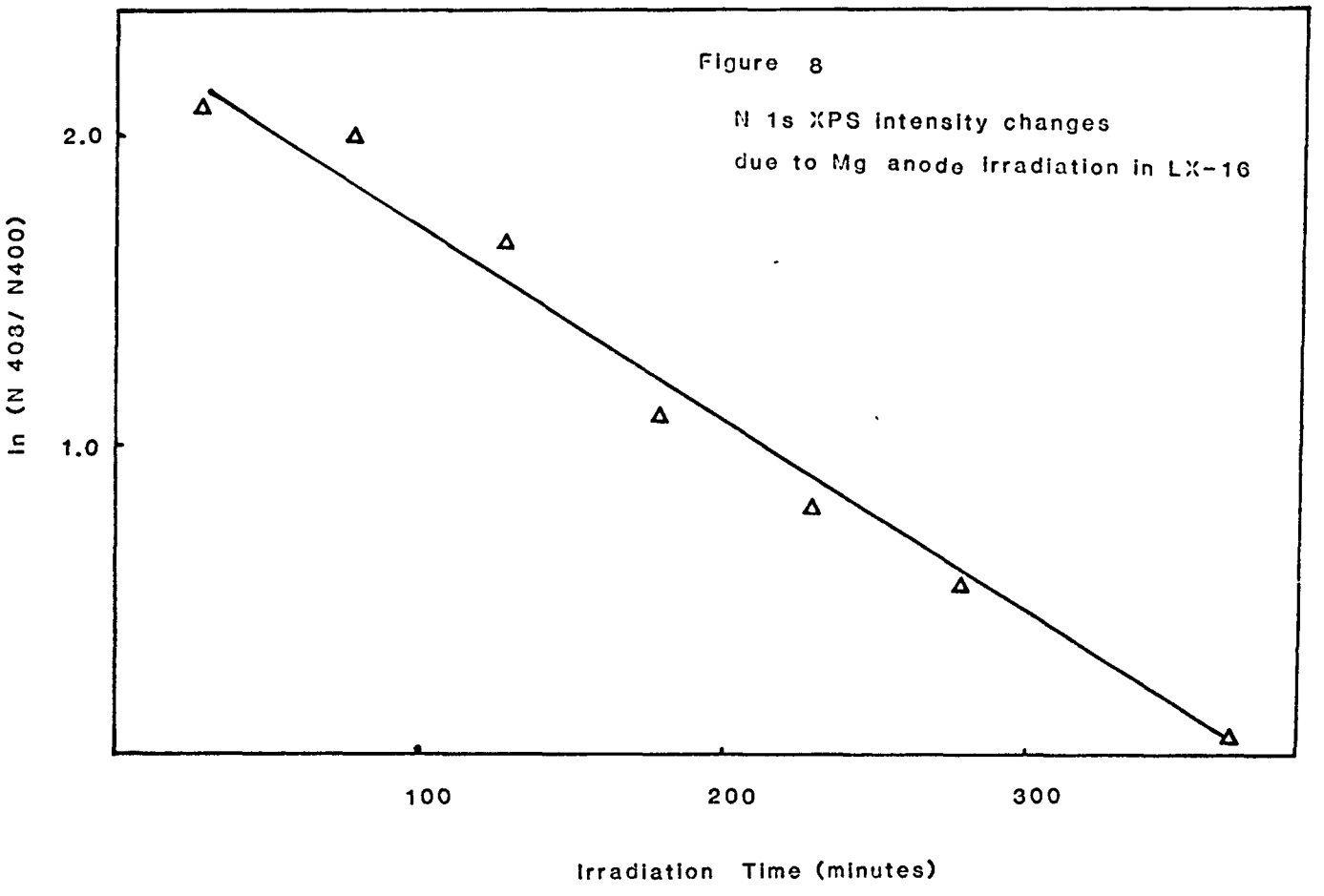
Figure 8
N 1s XPS intensity changes
due to Mg anode irradiation in LX-16
ln (N 403/ N400)
2.0
1.0
100
200
300
Irradiation Time (minutes)

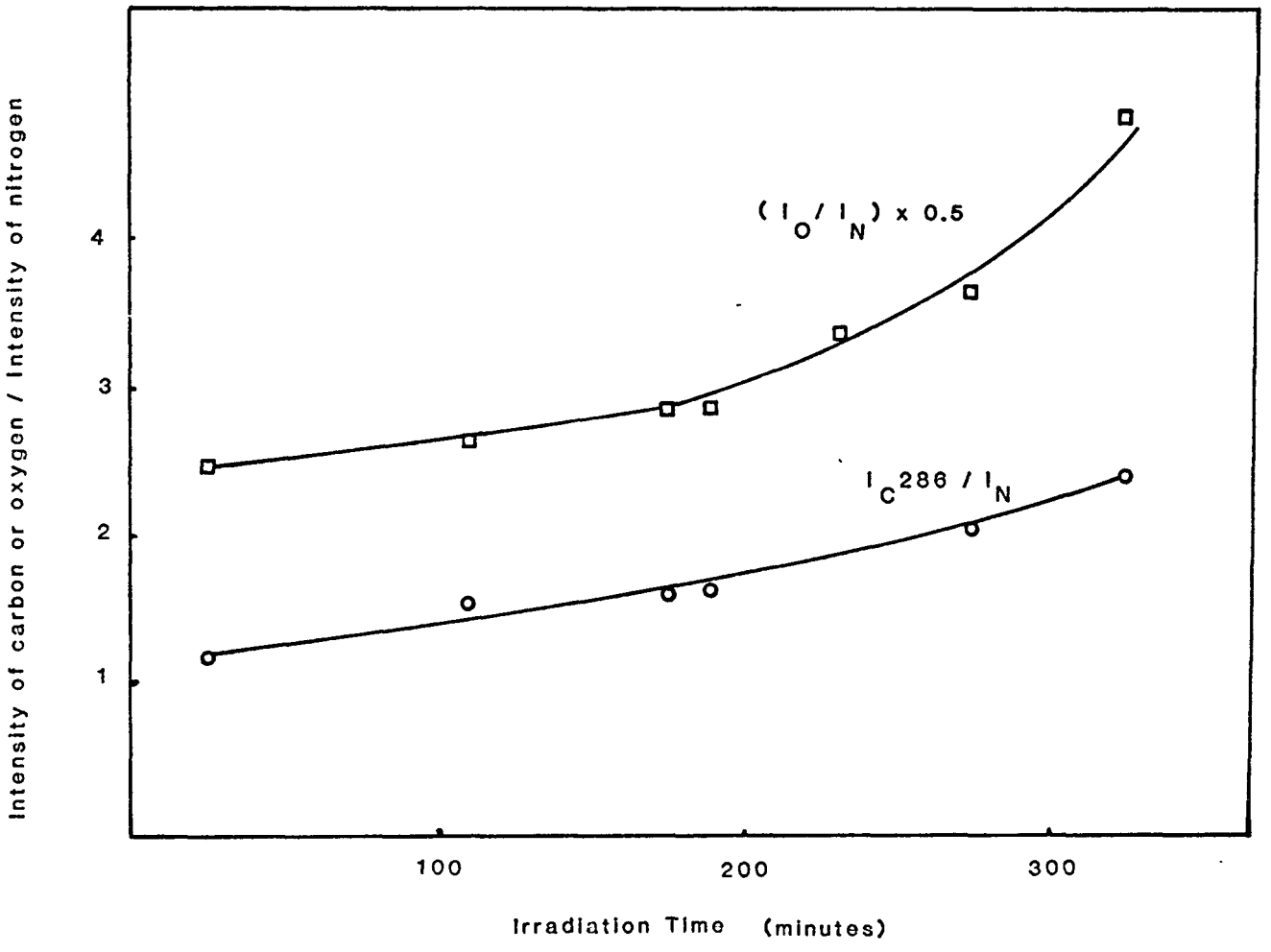

Figure 9 Nitrogen decrease in LX-16 during x-irradiation

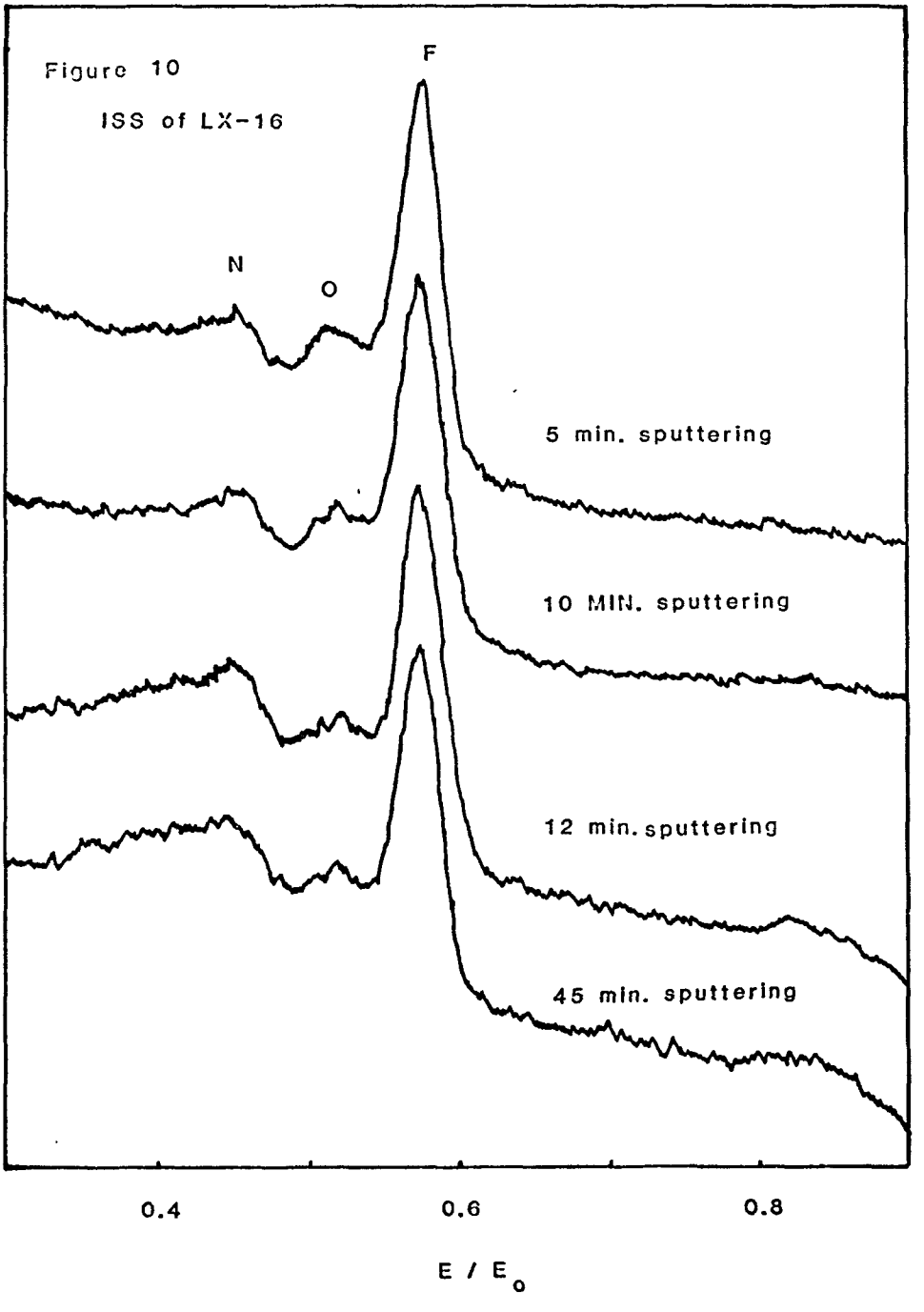
Figure 10
ISS of LX-16
F
N
O
5 min. sputtering
10 MIN. sputtering
12 min. sputtering
45 min. sputtering
0.4
0.6
0.8
E / E o

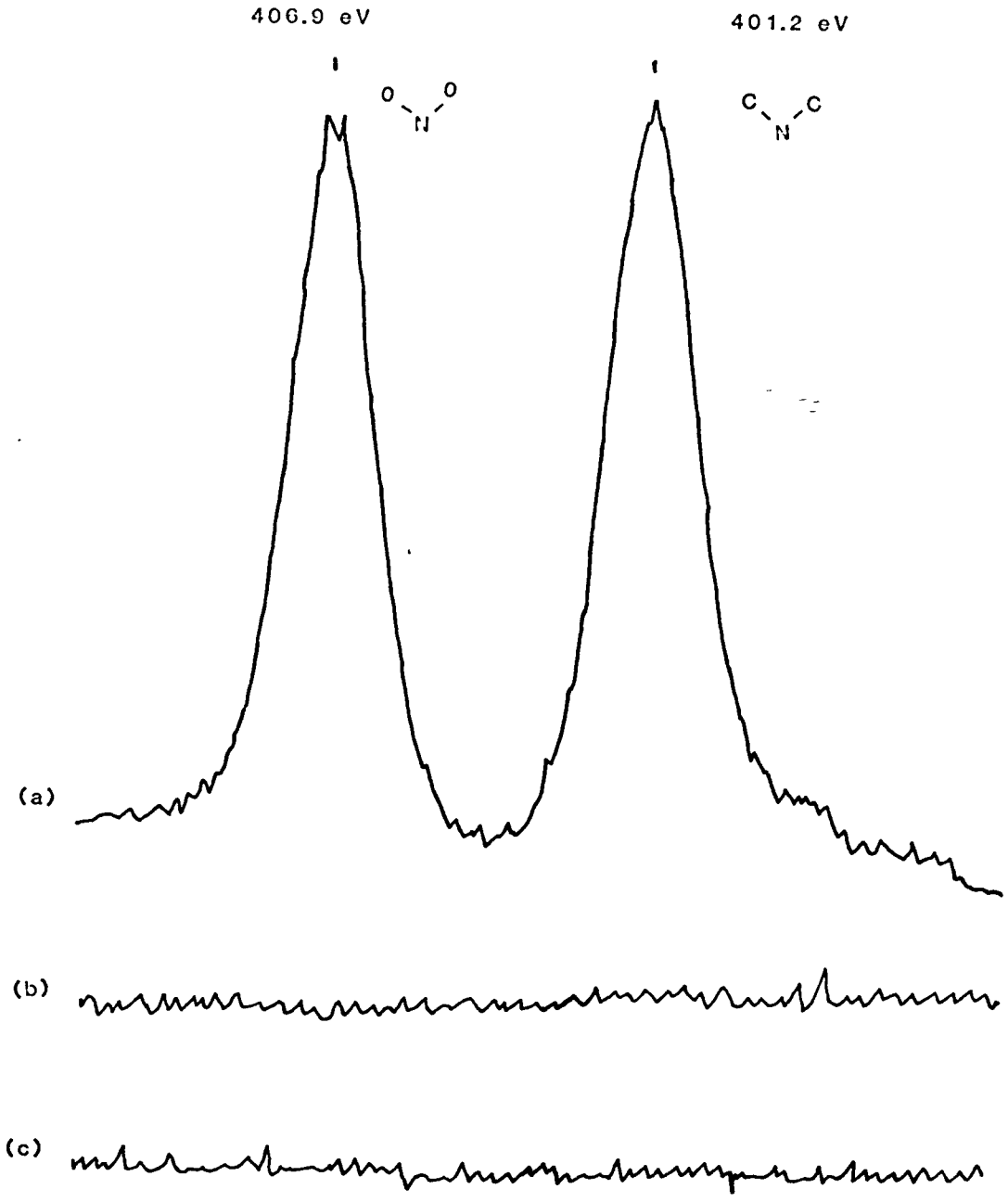

Figure 11 N 1s XPS spectra of (a) RDX

(b) PBX-9407

(c) FPC 461

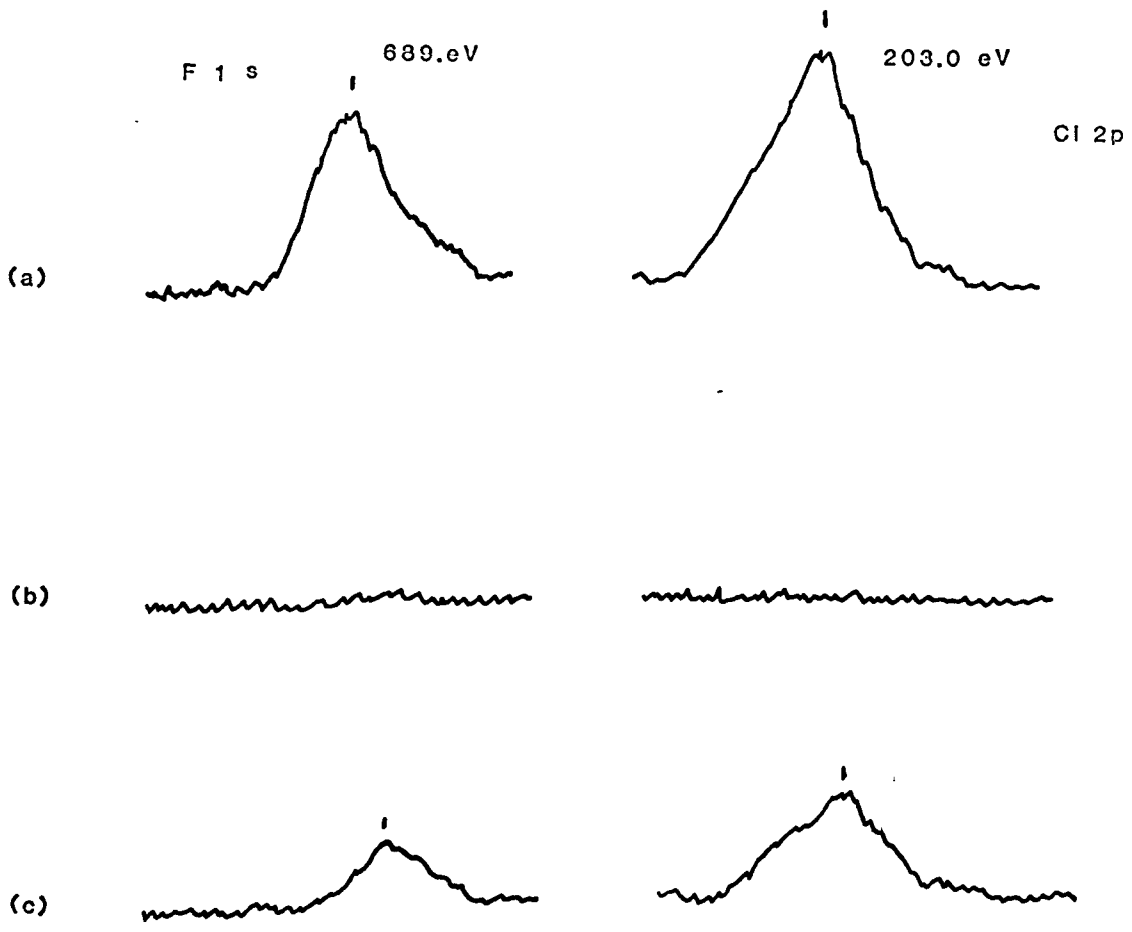

Figure 12 Cl 2p and F 1s XPS spectra of (a) FPC 461
(b) RDX
(c) PBX - 9407